Research Square

Preprints are preliminary reports that have not undergone peer review.
They should not be considered conclusive, used to inform clinical practice,
or referenced by the media as validated information.

Development and characterization of FI 7500: a novel near-infrared dye for in vitro and in vivo cell labeling

Takuya Ono

takuya.ono@artiencegroup.com

artience Co., Ltd. https://orcid.org/0000-0002-0960-3532

Airi Nakano

National Cancer Center Research Institute

Daiki Inomata

artience Co., Ltd

Hiroaki Kawauchi

artience Co., Ltd.

Yusuke Sakai

National Cancer Center Research Institute

Kassai Hidetoshi

National Cancer Center Research Institute

Hidenori Minashima

artience Co., Ltd.

Research Article

Keywords: near-infrared dye, spheroid, mouse model, cancer metastasis, cell tracing

Posted Date: November 13th, 2026

DOI: https://doi.org/10.21203/rs.3.rs-11560724/v1

License: This work is licensed under a Creative Commons Attribution 4.0 International License.
Read Full License

1 Introduction

Cell staining is a fundamental technique in which specific dyes are used to label and visualize cells and their internal structures [1, 2]. This approach is widely employed to evaluate cellular morphology, size, and function, and is indispensable in various fields, including cell biology, pathology, and developmental biology [3,4]. Several cell-staining dyes are currently commercially available and can be classified by their staining targets, functional properties, and spectral characteristics [5].

Recently, fluorescent dyes that absorb in the near-infrared (NIR) region, particularly in the 650–2000 nm range, have attracted considerable attention [6,7]. Compared with visible light, NIR light exhibits reduced scattering and absorption in biological tissues, allowing more efficient penetration through the skin and deep tissues and thereby enabling superior in vivo imaging [8]. Microscopy techniques operating in the NIR region, including confocal, multiphoton, and light-sheet microscopy, have been actively developed owing to advances in fluorescence imaging technologies [8, 9].

Currently, in vivo imaging in small animals relies predominantly on bioluminescence imaging using luciferase-expressing cells in combination with substrates such as luciferin [10, 11]. While effective, this approach has several limitations: it requires genetic modification of cells and repeated substrate administration throughout the experiment, and it raises concerns about the potential physiological effects of luciferin on animals [12,13]. These drawbacks increase both experimental complexity and cost, highlighting the need for alternative imaging modalities.

Therefore, establishing fluorescent dye-based in vivo imaging as a viable alternative could address many of these limitations. However, only a few NIR fluorescent dyes have been sufficiently validated for in vivo applications, and systematic characterization is essential to establish their utility and guide appropriate selection for specific experimental needs.

The NIR dye FI 7500 possesses a phthalocyanine structure (Online Resource 1), which endows it with superior photostability, thus offering the potential to overcome key limitations of conventional dyes [15,16]. However, its in vitro properties and detailed performance have not yet been systematically characterized. Here, we present a comprehensive in vitro characterization of FI 7500, including its staining performance in two-dimensional (2D) and three-dimensional (3D) cell culture models, and assess its suitability for in vivo applications via subcutaneous and intravenous administration of FI 7500-stained cells. This characterization will contribute to expanding the choice of NIR dyes for cellular and in vivo imaging, facilitating more informed selection of fluorescent probes for specific experimental requirements.

2 Materials and methods

2.1 Dye solution preparation

To dissolve FI 7500, 50 µL of dimethyl sulfoxide (DMSO; spectroscopic grade; FUJIFILM Wako Pure Chemical Co., Osaka, Japan) was added to the tube containing the dye powder. The final concentration of the FI 7500 solution was 200 µM.

2.2 Spectral properties

The absorption and fluorescence spectra of FI 7500 were measured using an ultraviolet–visible–NIR spectrophotometer UH5700 (Hitachi High-Tech Corp., Tokyo, Japan) and a spectrofluorometer FP-6500 (JASCO Corp., Tokyo, Japan), respectively. The 200 μM stock solution was diluted 10-fold to obtain a 20 μM solution, followed by an additional 10-fold dilution to a final concentration of 2 μM for spectral measurements. All measurements were performed using the diluted dye solutions under standard instrument settings.

2.3 Cytotoxicity analysis of FI 7500

To evaluate the cytotoxicity of FI 7500 and determine an appropriate staining concentration, HeLa cells (2×10^4 cells/well) were seeded in a 96-well plate (Thermo Fisher Scientific Inc., Waltham, MA, USA) and maintained in low-glucose Dulbecco's modified Eagle medium (DMEM; FUJIFILM Wako Pure Chemical Co.) supplemented with 10% heat-inactivated fetal bovine serum (FBS; Serana Europe GmbH, Brandenburg, Germany), 100 μg/mL penicillin, and 100 μg/mL streptomycin (Thermo Fisher Scientific Inc.) at 37 °C in a humidified atmosphere containing 5% CO_2. The day after cell seeding, the cells were incubated with 0, 0.05, 0.1, 0.2, 0.3, and 1 μM FI 7500 for 30 min at 37 °C in a humidified atmosphere containing 5% CO_2. After staining, the cells were cultured for 24 or 48 h, and cell viability was then measured using the Cell Counting Kit-8 (CCK-8) reagent (Dojindo Molecular Technologies Inc.,

Kumamoto, Japan) according to the manufacturer's protocol. Growth inhibition (%) was calculated relative to that in the DMSO-treated control.

2.4 Optimal staining time identification

To identify the optimal staining time for FI 7500, HeLa cells (2×10^4 cells/well) were seeded in a 96-well plate (Thermo Fisher Scientific Inc.) and maintained under the conditions mentioned above. Upon reaching sub-confluence, the cells were treated with 0.2 μM FI 7500 at 37 °C in a humidified incubator containing 5% CO_2 and were imaged every 5 min for 45 min using a BZ-X 800 microscope (KEYENCE Co., Osaka, Japan) with a Cy5 band-pass filter.

2.5 Staining site identification

To identify the subcellular localization of FI 7500, HeLa cells were seeded onto 10-cm cell culture dishes (Wuxi NEST Biotechnology Co., Ltd., Jiangsu, China) and maintained under the conditions mentioned above. Upon reaching sub-confluence, the cells were treated with 0.2 μM FI 7500 for 30 min at 37 °C in a humidified incubator containing 5% CO_2, stained using ER-Tracker™ Green (Thermo Fisher Scientific Inc.) or MitoTracker™ Orange FM (Thermo Fisher Scientific Inc.) according to the manufacturer's instructions, and observed under a BZ-X 800 microscope using appropriate band-pass filters selected for each dye. The degree of colocalization was quantified by image analysis using ImageJ software.

74

75 ***2.6 Cell staining (2D)***

76 To evaluate the 2D cell staining ability of FI 7500, HeLa, C2C12, NIH/3T3, Hep G2, HuH-7, and A-431
77 cells were seeded onto 10-cm cell culture dishes and maintained under the conditions mentioned above.
78 Upon reaching sub-confluence, the cells were treated with 0.2 μM FI 7500 for 30 min at 37 °C in a
79 humidified incubator containing 5% CO_2, washed three times with phosphate-buffered saline [PBS (−);
80 FUJIFILM Wako Pure Chemical Co.], and observed under a BZ-X 800 microscope with a Cy5 band-pass
81 filter.
82 NIH/3T3 cells grown on an 8-well glass chamber plate (NIPPON Genetics Co., Ltd., Tokyo, Japan) were
83 fixed with Mildform® 10N (FUJIFILM Wako Pure Chemical Co.) for 15 min at room temperature and
84 washed three times with PBS. The cells were blocked with 1% bovine serum albumin (FUJIFILM Wako
85 Pure Chemical Co.) in PBS for 60 min at room temperature. The cells were incubated for 60 min at room
86 temperature with Phalloidin-iFluor® 532 Conjugate (Cayman Chemical Co., MI, USA; diluted 1:500) and
87 Hoechst 33342 (DOJINDO LABORATORIES, Kumamoto, Japan; diluted 1:1000). After three washes with
88 PBS, the cells were incubated with FI 7500 for 30 min at 37 °C. Images were acquired with a BZ-X 800
89 microscope using appropriate band-pass filters selected for each dye.
90

91 ***2.7 Cell staining (3D)***

92 ***2.7.1 Cross-section staining***

93 To evaluate the spheroid cross-section staining ability of FI 7500, NIH/3T3 cells were seeded onto 10-cm
94 cell culture dishes and maintained under the conditions mentioned above. Upon reaching sub-confluence,
95 the cells were treated with 0.2 μM FI 7500 for 30 min at 37 °C in a humidified incubator containing 5%
96 CO_2, washed three times with PBS (−), and dissociated using trypsin–ethylenediaminetetraacetic acid
97 (EDTA) solution (Thermo Fisher Scientific Inc.). Subsequently, they were transferred to a 96-well, clear,
98 U-bottom, ultra-low-attachment microplate (Sumitomo Bakelite Co., Ltd., Shinagawa-ku, Tokyo, Japan) at
99 a density of 5×10^2, 1×10^3, 2×10^3, 3×10^3, 4×10^3, 5×10^3, and 1×10^4 cells/well and maintained at 37 °C in a
100 humidified incubator containing 5% CO_2. After two days, the spheroids were transferred to an 8-well glass
101 chamber plate, and images were acquired using a BZ-X 800 microscope with an appropriate band-pass
102 filter.

103 Then, the spheroids fabricated with 5×10^3 and 1×10^4 cells were fixed using Mildform® 10N at room
104 temperature for 60 min, washed with PBS (−), and cleared by overnight incubation with SCALEVIEW-S4
105 (FUJIFILM Wako Pure Chemical Co.) at 37 °C in a humidified incubator containing 5% CO_2 *[17]*. The
106 cleared spheroids were transferred to an 8-well glass chamber plate, and images were acquired using a BZ-
107 X 800 microscope with an appropriate band-pass filter.

108

109 ***2.7.2 Surface staining***

To evaluate the spheroid surface staining ability of FI 7500, NIH/3T3 cells were cultured under the conditions mentioned above. Upon reaching sub-confluence, the cells were washed with PBS (−) and dissociated using trypsin–EDTA solution (Thermo Fisher Scientific Inc.). Subsequently, they were transferred to a 96-well, clear, U-bottom, ultra-low-attachment microplate (Sumitomo Bakelite Co., Ltd.) at a density of 5×10^3 cells/well and maintained at 37 °C in a humidified incubator containing 5% CO_2. After two days, the spheroids were treated with 0.2 μM FI 7500 for 30 min at 37 °C in a humidified incubator containing 5% CO_2 and washed three times with PBS (−). The stained spheroids were transferred to an 8-well glass chamber plate, and images were acquired using a BZ-X 800 microscope with an appropriate band-pass filter.

2.8 Subcutaneous injection

To assess the in vivo fluorescence retention of FI 7500, 1×10^6 or 2×10^6 HeLa cells stained with 0.2 μM FI 7500 were mixed with an equal volume of Matrigel (Corning Inc., Corning, NY, USA). The cell suspension was subcutaneously injected into 7-week-old female BALB/cAJcl-nu/nu mice (CLEA Japan Inc., Tokyo, Japan) using a 1-mL syringe (Terumo Corp., Tokyo, Japan) and a 27 G needle (Terumo Corp.). The body weight and tumor size of the mice were measured three times per week. At the same time points, the fluorescence intensity of the transplanted cells was measured using an IVIS-Spectrum (Summit Pharmaceuticals International Corp., Tokyo, Japan). The animal experiments were conducted in compliance

with the guidelines of the Institute for Laboratory Animal Research, National Cancer Center Research Institute (approval no. T25-006).

2.9 Intravenous injection

To assess the in vivo cell tracking capability of FI 7500, 5×10^6 B16-F10/EF1a-Luc cells stained with 0.2 μM FI 7500 were suspended in 200 μL of DMEM. The cell suspension was intravenously injected into the tail vein of 7-week-old female BALB/cAJcl-nu/nu mice (CLEA Japan Inc.) using a 1-mL syringe (Terumo Corp.) and a 27 G needle (Terumo Corp.). The fluorescence intensity of the transplanted cells was measured using an IVIS-Spectrum (Summit Pharmaceuticals International Corp.). D-Luciferin (Summit Pharmaceuticals International Corp.) was prepared at 30 mg/mL in PBS and injected intraperitoneally at a dose of 150 mg/kg body weight prior to each bioluminescence imaging session.

The animal experiments were conducted in compliance with the guidelines of the Institute for Laboratory Animal Research, National Cancer Center Research Institute (approval no. T25-006).

3 Results

3.1 Characterization of FI 7500

To evaluate the photophysical properties of FI 7500, its absorption and fluorescence spectra were measured (Fig. 1). The absorption spectrum displayed a sharp and maximum absorption maximum in the NIR region

146 at approximately 714 nm, along with minor shoulder absorption bands at approximately 300 and 460 nm
147 (Fig. 1a). Upon excitation at its maximum absorption wavelength, FI 7500 exhibited a distinct fluorescence
148 spectrum centered at approximately 725 nm (Fig. 1b). The dye demonstrated a stokes shift of approximately
149 10 nm, indicating minimal structural rearrangement in the excited state and favorable properties for optical
150 imaging with reduced self-absorption.
151 Phase-contrast images and CCK-8 assay results indicated that FI 7500 was cytotoxic at concentrations
152 exceeding 0.3 μM (Online Resource 2). Therefore, we used FI 7500 at a concentration of 0.2 μM for staining
153 in subsequent experiments.
154 To determine the optimal incubation time for cellular staining, fluorescence intensity was monitored over
155 time using a fluorescence microscope (Online Resource 3). The signal intensity increased progressively
156 and reached a plateau after 30 min, with no change observed at later time points. Based on these
157 observations, 30 min was selected as the optimal staining time for subsequent experiments.
158 Microscopic observation and image analysis revealed that FI 7500 localized to the endoplasmic reticulum
159 (ER), as shown by its co-staining with ER-Tracker, an ER-specific dye (Fig. 1c, d). Moreover, in different
160 cell lines, FI 7500 staining showed strong fluorescence in the cytoplasm, where the ER is located, whereas
161 the nuclei were not stained (Fig. 2a). In elongated cells such as C2C12, FI 7500 enabled clear staining
162 extending to the cell periphery (Fig. 2a). FI 7500 could also be combined with phalloidin and Hoechst
163 33342 for multicolor staining of NIH/3T3 cells (Fig. 2b).

3.2 Observation of stained cells (3D)

To evaluate the applicability of FI 7500 for 3D cell culture imaging, we stained spheroids containing different numbers of cells and observed them under a microscope. Under live-cell conditions without fixation or clearing, FI 7500 enabled visualization of the internal structure of spheroids containing up to 2×10^3 cells (Online Resource 4). After optical clearing of fixed spheroids, the penetration depth was further improved, enabling internal visualization of spheroids containing up to 1×10^4 cells (Fig. 3a, b). However, dye penetration in larger spheroids ($>1\times10^4$ cells) remained limited even after clearing, and the central regions were undetectable (data not shown).

In addition to internal imaging, FI 7500 enabled observation of the spheroid surface. High-resolution microscopy revealed the characteristic staining pattern of FI 7500, in which the cytoplasm was labeled while the nuclei remained unstained, clearly delineating individual cells at the spheroid surface (Fig. 3c, d).

3.3 In vivo observation of stained cells

After subcutaneous transplantation of FI 7500-stained HeLa cells (Fig. 4a), we observed that FI 7500 retained fluorescence in the mice until day 21, regardless of the number of transplanted cells. However, after day 21, the fluorescence intensity decreased first in the group transplanted with fewer cells (Fig. 4b, c), and by day 28, the signals in both groups had fallen below the detection limit (data not shown). The

tumor growth curves were comparable between mice transplanted with unstained and FI 7500-stained cells (Online Resource 5).

After intravenous transplantation of FI 7500-stained B16-F10/EF1a-Luc cells (Fig. 5a), we confirmed the successful in vivo tracking of the transplanted cells. Specifically, the cells accumulated in the lungs, where they were continuously monitored for 3 h (Fig. 5b).

4 Discussion

In this study, we comprehensively characterized the NIR fluorescent dye FI 7500 for in vitro and in vivo imaging applications. Although FI 7500 is a promising tool for cell staining, its detailed in vitro properties had not been systematically evaluated. Our characterization, including staining performance in 2D and 3D cell culture models and in vivo imaging after subcutaneous and intravenous administration of stained cells, demonstrates its potential as a reliable alternative to bioluminescence imaging, which requires genetic modification and repeated substrate administration.

Before evaluating the in vivo performance of FI 7500, we characterized its photophysical properties and validated its feasibility for in vitro cellular imaging. Based on the spectral measurements, FI 7500 is suitable for observation with Cy5, Cy5.5, and Cy7 band-pass filters. FI 7500 also offers a distinct advantage for multicolor staining, as its emission spectrum does not overlap with those of conventional visible-light fluorophores [5]. Our microscopy-based analysis revealed that FI 7500 specifically localizes to the ER, as

demonstrated by co-staining with ER-Tracker and subsequent image analysis. This ER-specific localization pattern was consistently observed across multiple cell types, with strong cytoplasmic fluorescence and no nuclear staining. Notably, in elongated cells such as C2C12 myoblasts, FI 7500 enabled clear visualization of ER networks extending to the cell periphery, suggesting its utility for visualizing cellular morphology in cells with complex shapes [18]. Its distribution throughout the cytoplasm enables whole-cell visualization without nuclear interference, which is particularly valuable for tracking cell migration and morphological changes.

As a preliminary step toward in vivo studies, we focused on evaluating whether FI 7500 could facilitate deep fluorescence visualization within in vitro 3D cellular structures, thereby assessing its suitability for thick biological samples. Our 3D imaging analysis demonstrated that FI 7500 can visualize spheroid structures under multiple conditions, with penetration depth depending on sample preparation. Under live-cell conditions, internal structures were observable in spheroids containing up to 2×10^3 cells, whereas optical clearing extended this capability to spheroids containing 1×10^4 cells [19,20]. Beyond this size, the central regions remained undetectable, possibly owing to insufficient penetration of excitation light into the core or reduced detection efficiency of fluorescence emitted from the inner regions.

Furthermore, FI 7500 was effective for surface imaging regardless of spheroid size, with its ER-specific staining pattern clearly delineating individual cells at the periphery. This surface imaging capability is particularly valuable because the spheroid periphery represents the most metabolically active region and

218 the primary site of interaction with the microenvironment [21,22]. The ability to perform live-cell imaging
219 without fixation or clearing enables real-time monitoring of dynamic processes such as proliferation,
220 migration, and drug response in 3D models [22,23]. Collectively, these findings position FI 7500 as a
221 versatile tool that can be adapted to different experimental needs: live-cell imaging for small spheroids,
222 clearing-enhanced imaging for medium-sized spheroids, and high-resolution surface analysis for larger
223 structures.

224 Based on these findings, which confirmed the fundamental properties and performance of FI 7500 in
225 monolayer and 3D cellular environments, we subsequently proceeded to in vivo evaluation. In vivo
226 validation of subcutaneously injected FI 7500-stained cells showed that the tumor diameter increased
227 gradually over time, whereas the fluorescent area progressively decreased (Fig. 4a, b). We initially
228 hypothesized that the fluorescent area would correspond to the tumor area, enabling the use of fluorescence
229 data for tumor size measurement. However, the results of this validation suggest that this approach is not
230 feasible. The reduction in fluorescent area may be attributed to photobleaching caused by continuous
231 exposure to fluorescent lights in the animal facility, metabolic degradation within the mouse body, and
232 quenching below the detection limit due to cell division [24,25], although the precise mechanism remains
233 unclear.

234 Before the subcutaneous transplantation experiment, we were concerned that FI 7500 toxicity might
235 inhibit tumor formation. However, the tumor growth curves were comparable between mice transplanted

with unstained and stained cells (Online Resource 5). Therefore, we concluded that the effect of FI 7500 on tumor formation was negligible.

B16-F10/EF1a-Luc is a melanoma cell line known to metastasize to the lungs upon intravenous administration in animal models [26,27]. In this study, FI 7500-stained cells administered via the tail vein accumulated in the lungs after transplantation, demonstrating behavior consistent with that observed in the luciferin-administered group. While tracking cellular metastatic dynamics has conventionally relied on luciferin administration in combination with luciferase-expressing cells [28,29], our findings demonstrate that fluorescent dyes such as FI 7500 can also serve as a highly effective tool for tracking tumor metastasis.

Although bioluminescence imaging with D-luciferin is a standard method, it has several practical limitations. First, repeated administration of luciferin prior to every imaging session is time-consuming and costly, especially when handling large cohorts of mice. Second, this approach requires luciferase-expressing cells, which necessitates additional time and resources to purchase or establish stable cell lines if they are not readily available. In contrast, cell staining with FI 7500 requires only a brief 30-min incubation before transplantation, enabling convenient in vivo monitoring in fluorescence mode without the need for repeated substrate injections. Therefore, in vivo imaging with FI 7500 offers a highly practical alternative to bioluminescence imaging, serving as a powerful and versatile new experimental tool for researchers.

This study has several limitations. First, although FI 7500 demonstrated ER-specific localization and effective staining in multiple cell types, we did not systematically compare its performance with other

commercially available NIR dyes such as DiD and DiR under identical experimental conditions [30]. Such comparative analyses would provide valuable insights into the relative advantages and disadvantages of FI 7500 for specific applications. Second, although FI 7500 enabled the internal visualization of spheroids containing up to 1×10^4 cells after optical clearing, penetration remained limited in larger spheroids, restricting its utility for imaging dense 3D structures that more closely mimic in vivo tumor microenvironments [31,32]. This limitation may necessitate the use of complementary imaging modalities such as light-sheet microscopy or two-photon imaging for deep tissue penetration [33,34]. Future studies addressing these limitations should further refine the appropriate use of FI 7500 and guide the development of next-generation NIR fluorescent dyes with improved properties.

In summary, we characterized the NIR fluorescent dye FI 7500 for in vitro and in vivo imaging. FI 7500 localizes to the ER and enables the visualization of cell morphology in 2D and 3D cultures. It also enables long-term fluorescence retention in stained cells and real-time monitoring of metastatic cell accumulation in vivo, without adversely affecting tumor formation or growth. These findings support the use of FI 7500 as a practical alternative to bioluminescence imaging, eliminating the need for genetic modification and repeated substrate administration.

Acknowledgments

We thank Dr. Takashi Murakami (Saitama Medical University, Saitama, Japan) for providing the luciferase-

expressing cell line and Editage (www.editage.jp) for English language editing. This study was supported by the Fundamental Innovative Oncology Core of the National Cancer Center (Tokyo, Japan). We also thank National Cancer Center Research Institute Core Facility for in vivo imaging（IVIS-Spectrum, Summit Pharmaceuticals International Corp., Tokyo, Japan） in this study. The Core Facility was supported in part by National Cancer Center Research and Development Fund (2023-J-2).

Declarations

Funding

This study was financially supported in part by the National Cancer Center Research and Development Fund (no. 2026-J-02).

Conflicts of interest/Competing interests

This study was funded by artience Co., Ltd. Takuya Ono, Hiroaki Kawauchi, Daiki Inomata, and Hidenori Minashima are employees of artience Co., Ltd., which manufactures FI 7500, the dye used in this study. The authors hold a patent related to the technology described in this manuscript. The remaining authors declare no competing interests.

Ethics approval

The animal experiments were conducted in compliance with the guidelines of the Institute for Laboratory Animal Research, National Cancer Center Research Institute.

Informed consent

Not applicable

References

1. Alturkistani HA, Tashkandi FM, Mohammedsaleh ZM. Histological stains: a literature review and case study. Glob J Health Sci. 2015; 8:72. https://doi.org/10.5539/gjhs.v8n3p72

2. Titford M. Progress in the development of microscopical techniques for diagnostic pathology. J Histotechnol. 2009; 32:9–19. https://doi.org/10.1179/his.2009.32.1.9

3. Thul PJ, Åkesson L, Wiking M, et al. A subcellular map of the human proteome. Science. 2017; 356:eaal3321. https://doi.org/10.1126/science.aal3321

4. Fischer AH, Jacobson KA, Rose J, Zeller R. Hematoxylin and eosin staining of tissue and cell sections. Cold Spring Harb Protoc. 2008; 2008:pdb.prot4986. https://doi.org/10.1101/pdb.prot4986

5. Dsouza RN, Pischel U, Nau WM. Fluorescent dyes and their supramolecular host/guest complexes with macrocycles in aqueous solution. Chem Rev. 2011; 111:7941–80. https://doi.org/10.1021/cr200213s

6. Hong G, Antaris AL, Dai H. Near-infrared fluorophores for biomedical imaging. Nat Biomed Eng. 2017; 1:0010. https://doi.org/10.1038/s41551-016-0010

7. Kommidi SSR, Atkinson KM, Smith BD. Steric protection of near-infrared fluorescent dyes for enhanced bioimaging. J Mater Chem B. 2024; 12:8310–20. https://doi.org/10.1039/D4TB01281J

8. Weissleder R. A clearer vision for in vivo imaging. Nat Biotechnol. 2001; 19:316–7. https://doi.org/10.1038/86684

9. Helmchen F, Denk W. Deep tissue two-photon microscopy. Nat Methods. 2005; 2:932–40. https://doi.org/10.1038/nmeth818

10. Laissue PP, Alghamdi RA, Tomancak P, Reynaud EG, Shroff H. Assessing phototoxicity in live fluorescence imaging. Nat Methods. 2017; 14:657–61. https://doi.org/10.1038/nmeth.4344

11. Contag CH, Bachmann MH. Advances in in vivo bioluminescence imaging of gene expression. Annu Rev Biomed Eng. 2002; 4:235–60. https://doi.org/10.1146/annurev.bioeng.4.111901.093336

12. Sadikot RT, Blackwell TS. Bioluminescence imaging. Proc Am Thorac Soc. 2005; 2:537–40. https://doi.org/10.1513/pats.200507-067DS

13. Mezzanotte L, Van 'T Root M, Karatas H, Goun EA, Löwik CWGM. In vivo molecular bioluminescence imaging: new tools and applications. Trends Biotechnol. 2017; 35:640–52. https://doi.org/10.1016/j.tibtech.2017.03.012

14. Nakajima K, Hamada K, Ito R, et al. Stability of D-luciferin for bioluminescence to detect gene expression in freely moving mice for long durations. Luminescence. 2021; 36:94–8. https://doi.org/10.1002/bio.3917

15. Zheng Q, Lavis LD. Development of photostable fluorophores for molecular imaging. Curr Opin Chem Biol. 2017; 39:32–8. https://doi.org/10.1016/j.cbpa.2017.04.017

16. Sekkat N, Bergh HVD, Nyokong T, Lange N. Like a bolt from the blue: phthalocyanines in biomedical optics. Molecules. 2011; 17:98–144. https://doi.org/10.3390/molecules17010098

17. Boutin ME, Voss TC, Titus SA, Cruz-Gutierrez K, Michael S, Ferrer M. A high-throughput imaging and nuclear segmentation analysis protocol for cleared 3D culture models. Sci Rep. 2018; 8:11135. https://doi.org/10.1038/s41598-018-29169-0

18. Wu H, Carvalho P, Voeltz GK. Here, there, and everywhere: the importance of ER membrane contact sites. Science. 2018; 361:eaan5835. https://doi.org/10.1126/science.aan5835

19. Pampaloni F, Reynaud EG, Stelzer EHK. The third dimension bridges the gap between cell culture and live tissue. Nat Rev Mol Cell Biol. 2007; 8:839–45. https://doi.org/10.1038/nrm2236

20. Diosdi A, Hirling D, Kovacs M, et al. A quantitative metric for the comparative evaluation of optical clearing protocols for 3D multicellular spheroids. Comput Struct Biotechnol J. 2021; 19:1233–43. https://doi.org/10.1016/j.csbj.2021.01.040

21. Däster S, Amatruda N, Calabrese D, et al. Induction of hypoxia and necrosis in multicellular tumor spheroids is associated with resistance to chemotherapy treatment. Oncotarget. 2017; 8:1725–36. https://doi.org/10.18632/oncotarget.13857

22. Martinez NJ, Titus SA, Wagner AK, Simeonov A. High-throughput fluorescence imaging approaches for drug discovery using in vitro and in vivo three-dimensional models. Expert Opin Drug Discov. 2015; 10:1347–61. https://doi.org/10.1517/17460441.2015.1091814

23. Mikhail AS, Eetezadi S, Allen C. Multicellular tumor spheroids for evaluation of cytotoxicity and tumor

345 growth inhibitory effects of nanomedicines in vitro: a comparison of docetaxel-loaded block copolymer
346 micelles and Taxotere®. PLoS One. 2013; 8:e62630. https://doi.org/10.1371/journal.pone.0062630

347 24. Chung S, Kim S, Seo Y, Kim S, Lee JY. Quantitative analysis of cell proliferation by a dye dilution
348 assay: application to cell lines and cocultures. Cytometry A. 2017; 91:704–12.
349 https://doi.org/10.1002/cyto.a.23105

350 25. Progatzky F, Dallman MJ, Lo Celso C. From seeing to believing: labelling strategies for in vivo cell-
351 tracking experiments. Interface Focus. 2013; 3:20130001. https://doi.org/10.1098/rsfs.2013.0001

352 26. Fidler IJ. Biological behavior of malignant melanoma cells correlated to their survival in vivo. Cancer
353 Res. 1975; 35:218–24.

354 27. Shen K, Song W, Wang H, et al. Decoding the metastatic potential and optimal postoperative adjuvant
355 therapy of melanoma based on metastasis score. Cell Death Discov. 2023; 9:397.
356 https://doi.org/10.1038/s41420-023-01678-6

357 28. Zhu H, Kauffman M, Li J, et al. Innovative bioluminometric quantification of cancer cell load in target
358 organs: implications for studying anticancer drugs, including ROS enhancers. React Oxyg Species (Apex).
359 2016; 1:157–64. https://doi.org/10.20455/ros.2016.819

360 29. Adams ST, Miller SC. Beyond D-luciferin: expanding the scope of bioluminescence imaging in vivo.
361 Curr Opin Chem Biol. 2014; 21:112–20. https://doi.org/10.1016/j.cbpa.2014.07.003

362 30. Carlson AL, Fujisaki J, Wu J, et al. Tracking single cells in live animals using a photoconvertible near-
363 infrared cell membrane label. PLoS One. 2013; 8:e69257. https://doi.org/10.1371/journal.pone.0069257

364 31. Costa EC, Moreira AF, De Melo-Diogo D, Gaspar VM, Carvalho MP, Correia IJ. 3D tumor spheroids:
365 an overview on the tools and techniques used for their analysis. Biotechnol Adv. 2016; 34:1427–41.
366 https://doi.org/10.1016/j.biotechadv.2016.11.002

367 32. Costa EC, Silva DN, Moreira AF, Correia IJ. Optical clearing methods: an overview of the techniques
368 used for the imaging of 3D spheroids. Biotechnol Bioeng. 2019; 116:2742–63.
369 https://doi.org/10.1002/bit.27105

370 33. Susaki EA, Takasato M. Perspective: extending the utility of three-dimensional organoids by tissue
371 clearing technologies. Front Cell Dev Biol. 2021; 9:679226. https://doi.org/10.3389/fcell.2021.679226

372 34. Weiss KR, Voigt FF, Shepherd DP, Huisken J. Tutorial: practical considerations for tissue clearing and
373 imaging. Nat Protoc. 2021; 16:2732–48. https://doi.org/10.1038/s41596-021-00502-8

374

375

376 **Figure Legends**

377 **Fig. 1** Characteristics of FI 7500.

378 Absorption (a) and fluorescence (b) spectra of FI 7500 recorded in DMSO. Evaluation of the intracellular

379 staining site of FI 7500 via co-staining with MitoTracker and ER-Tracker (c) and the corresponding

380 colocalization measured using ImageJ (d)

381

382 **Fig. 2** Cell stainability of FI 7500.

383 The usability of FI 7500 in different cell lines was assessed by staining HeLa, Hep G2, HuH-7, NIH/3T3,

384 and C2C12 cells (a). The usability of FI 7500 for multiple staining was assessed by co-staining NIH/3T3

385 cells with phalloidin and Hoechst 33342 (b)

386

387 **Fig. 3** Spheroid stainability of FI 7500.

388 Schematic of the procedure for cross-section staining of spheroids with FI 7500 (a). Cross-sectional images

389 of spheroids containing 5×10^3 and 1×10^4 cells (b). Schematic of the procedure for surface staining of

390 spheroids with FI 7500 (c). Phase-contrast and FI 7500 fluorescence images of the surface of spheroids

391 containing 5×10^3 cells (d)

392

393 **Fig. 4** Subcutaneous implantation of FI 7500-stained cells.

394 Schematic of the procedure for subcutaneous implantation of FI 7500-stained HeLa cells (a). Time-

395 dependent changes in fluorescence intensity of FI 7500-stained HeLa cells transplanted at 1×10^6 cells (b)

396 and 2×10^6 cells (c), measured using an IVIS imaging system

397

398 **Fig. 5** Intravenous administration of FI 7500-stained cells.

399 Schematic of the procedure for intravenous administration of FI 7500-stained B16-F10/EF1a-Luc cells (a).

400 Time-dependent changes in fluorescence intensity of FI 7500-stained B16-F10/EF1a-Luc cells and

401 bioluminescence intensity following D-luciferin administration, measured using an IVIS imaging system

402 (b)

403

404 **Online Resource 1** Chemical structure of the phthalocyanine-based fluorescent dye FI 7500

405 **Online Resource 2** Cytotoxicity and cell proliferation assessment of FI 7500 in HeLa cells.

406 Phase-contrast images of HeLa cells treated with various concentrations of FI 7500 for 24 h (a) and 48 h

407 (b). Cell proliferation evaluated using the CCK-8 assay (c)

408 **Online Resource 3** Time-course imaging of FI 7500 in HeLa cells.

409 Representative fluorescence images of HeLa cells incubated with 0.2 μM FI 7500. Images were captured

410 every 5 min using a Cy5 band-pass filter

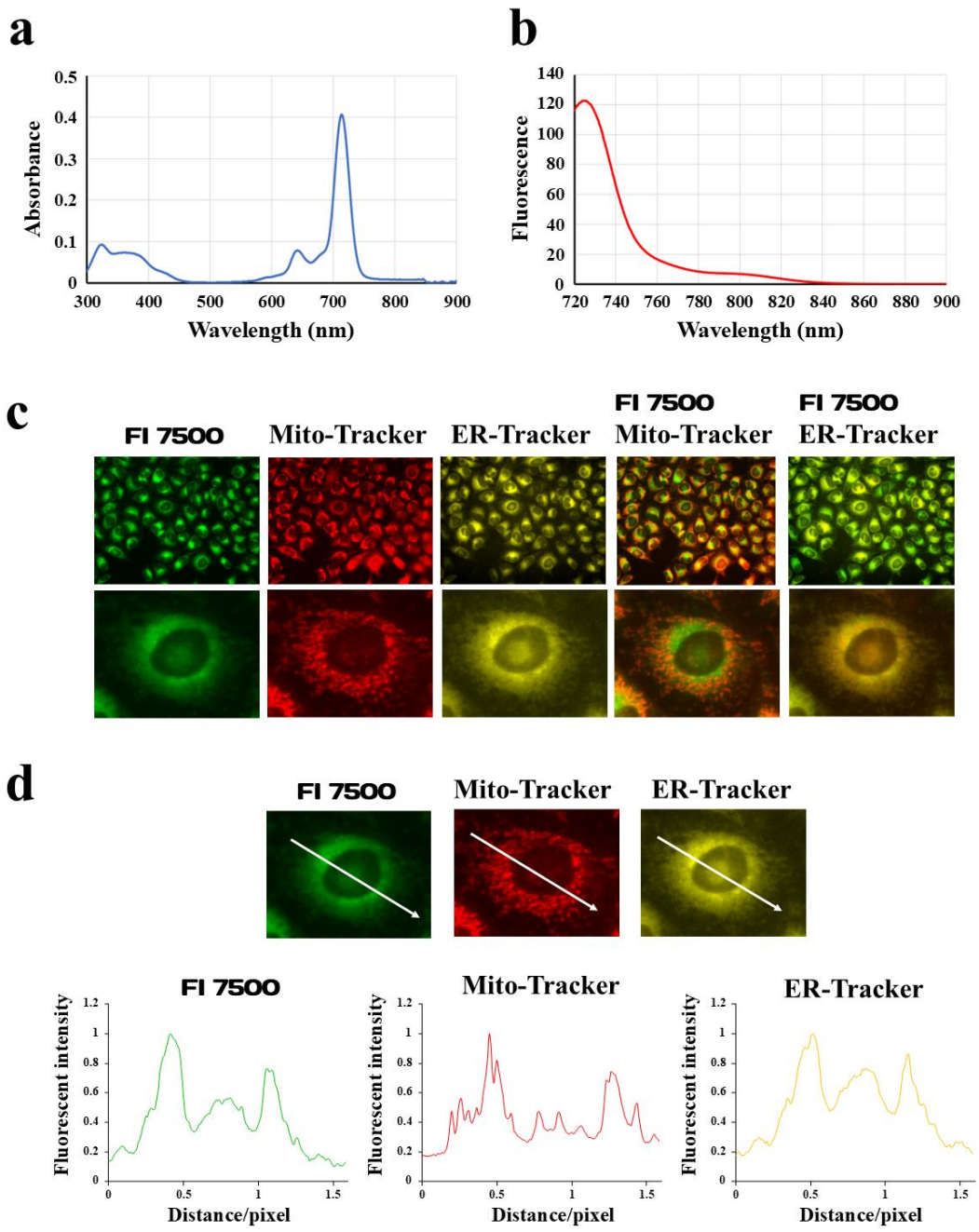
Online Resource 4 Cross-sectional images of live spheroids containing different numbers of cells stained with FI 7500.

Representative cross-sectional fluorescence images of live HeLa spheroids formed with various cell numbers (5×10^2, 1×10^3, 2×10^3, 3×10^3, 4×10^3, and 5×10^3 cells) following staining with 0.2 μM FI 7500. Images were acquired in the live state using confocal fluorescence microscopy with a Cy5 band-pass filter

Online Resource 5 Evaluation of the in vivo effect of FI 7500 on tumor growth.

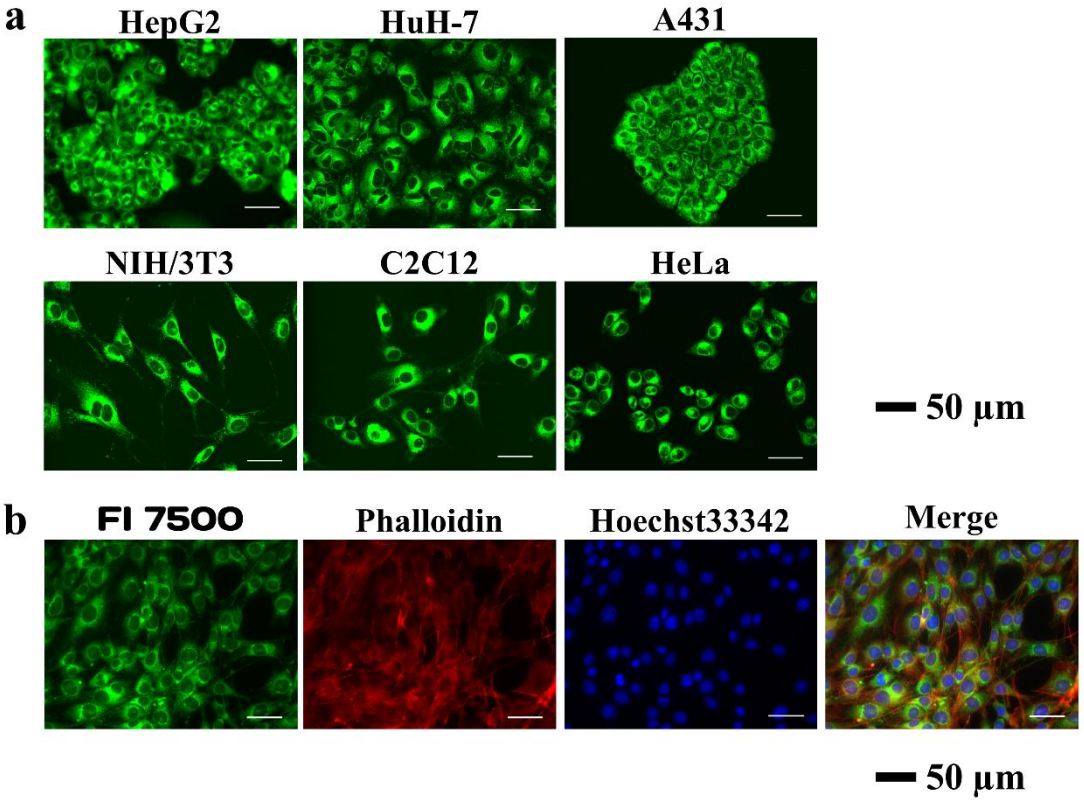
Evaluation of the in vivo effect of FI 7500 based on tumor diameter. FI 7500-stained or unstained HeLa cells were transplanted into mice at 1×10^6 or 2×10^6 cells/mouse, and time-dependent tumor growth was compared between the two groups

Figure 1


a
Absorbance
Wavelength (nm)
b
Fluorescence
Wavelength (nm)
c
FI 7500
Mito-Tracker
ER-Tracker
FI 7500
Mito-Tracker
FI 7500
ER-Tracker
d
FI 7500
Mito-Tracker
ER-Tracker
Fluorescent intensity
Distance/pixel
FI 7500
Mito-Tracker
ER-Tracker

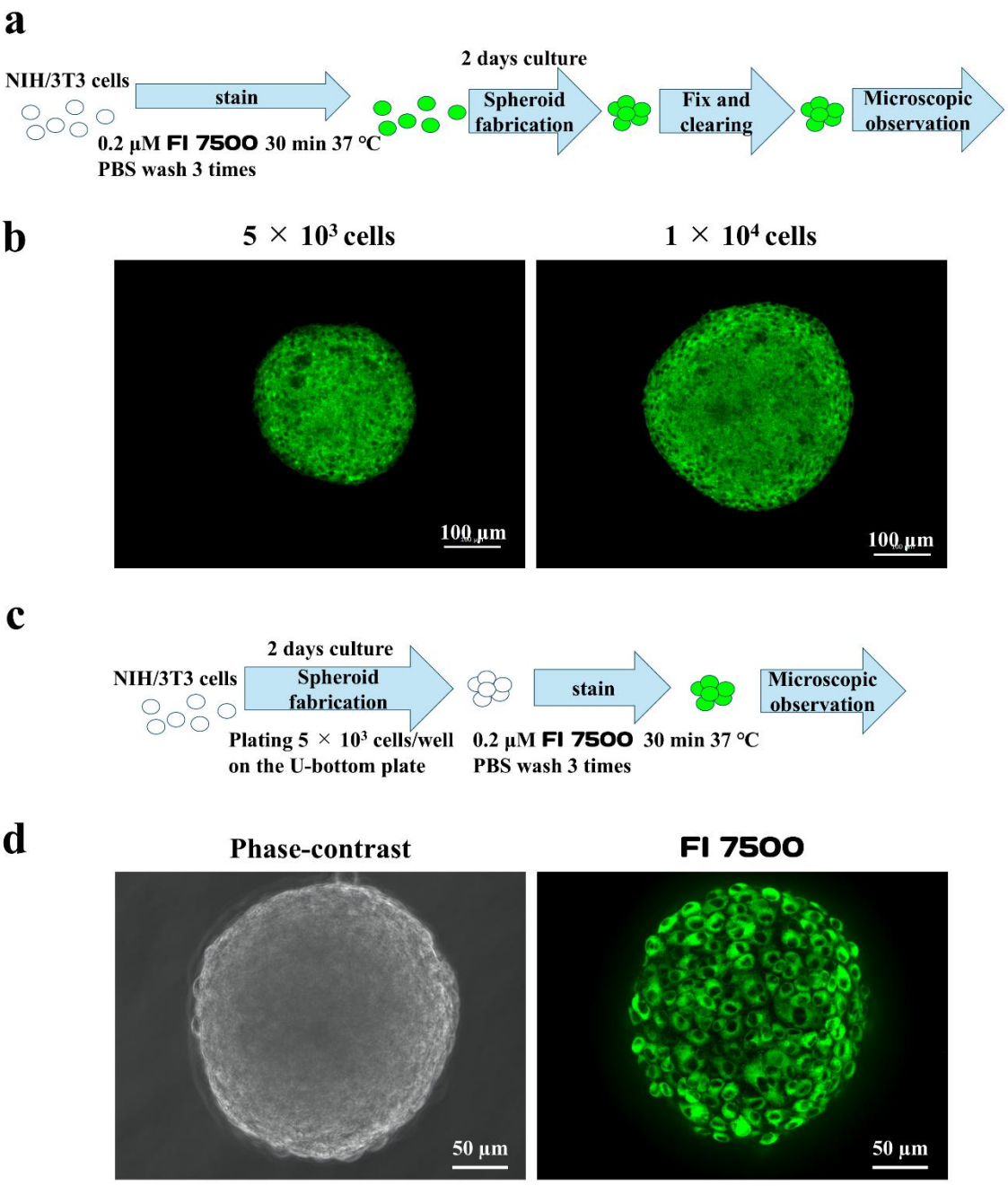
429

Figure 2


a
HepG2
HuH-7
A431
NIH/3T3
C2C12
HeLa
50 μm
b
FI 7500
Phalloidin
Hoechst33342
Merge
50 μm

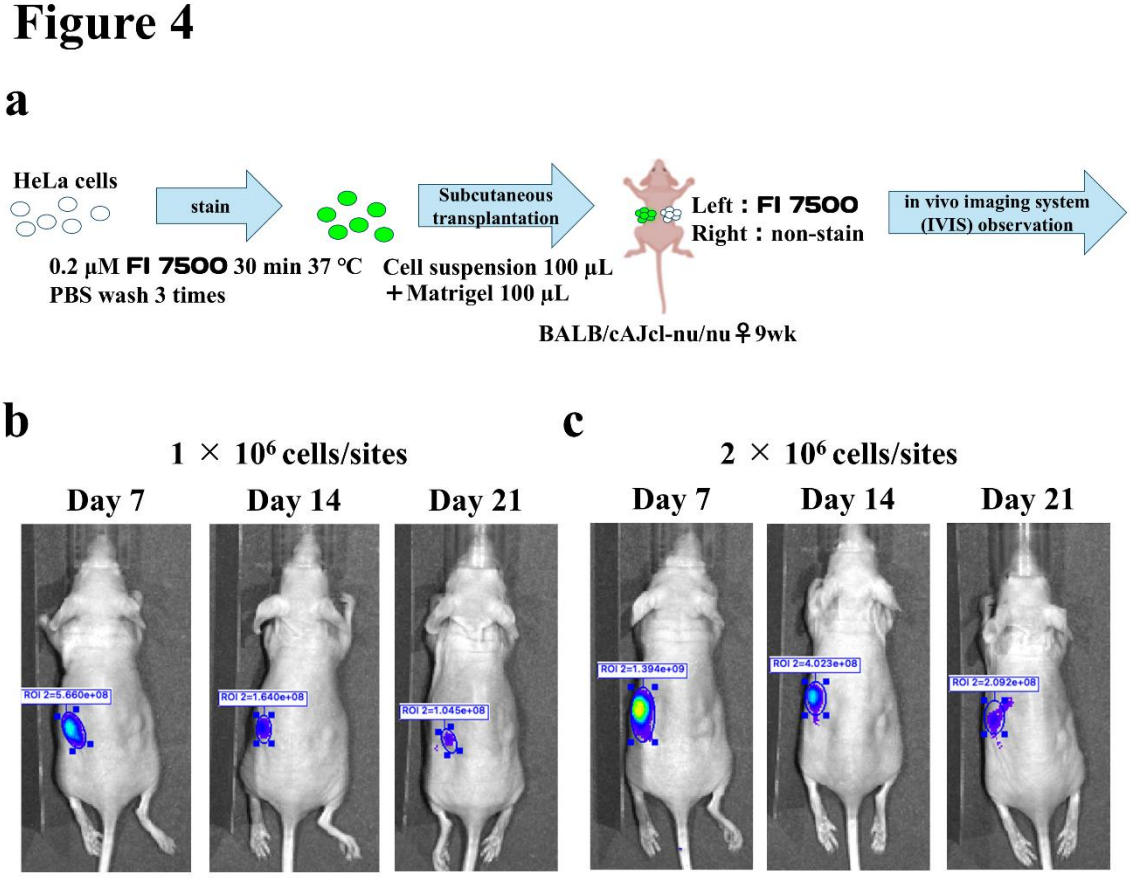
430

Figure 3


a
NIH/3T3 cells
stain
0.2 μM FI 7500 30 min 37 °C
PBS wash 3 times
2 days culture
Spheroid fabrication
Fix and clearing
Microscopic observation
b
5 × 10³ cells
1 × 10⁴ cells
100 μm
100 μm
c
NIH/3T3 cells
2 days culture
Spheroid fabrication
Plating 5 × 10³ cells/well on the U-bottom plate
stain
0.2 μM FI 7500 30 min 37 °C
PBS wash 3 times
Microscopic observation
d
Phase-contrast
FI 7500
50 μm
50 μm

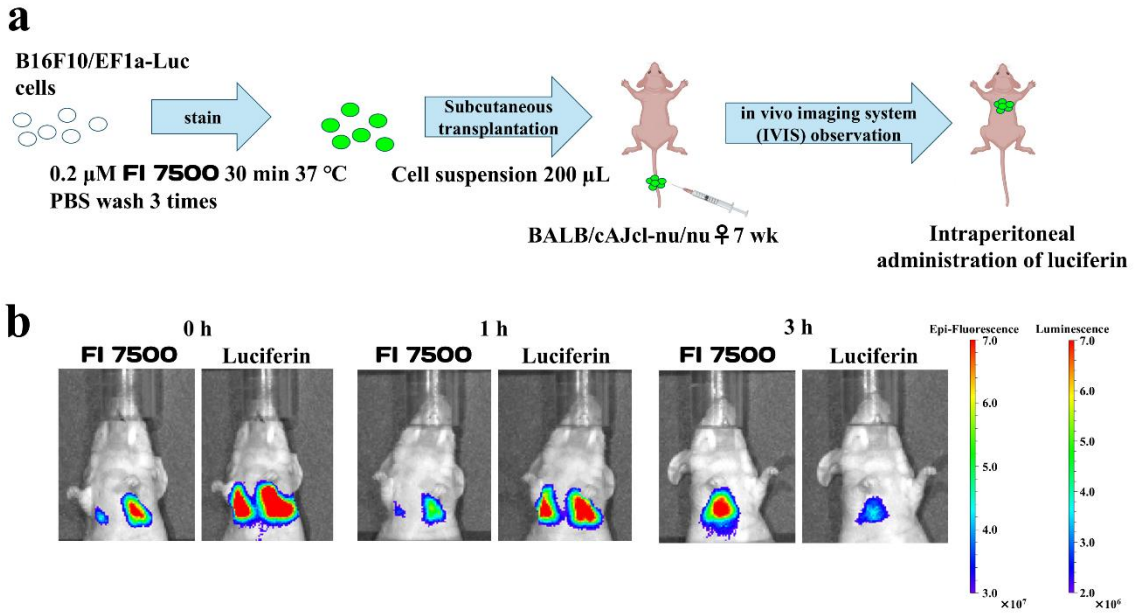
431

Figure 4


a
HeLa cells
stain
0.2 μM FI 7500 30 min 37 ℃
PBS wash 3 times
Cell suspension 100 μL
＋Matrigel 100 μL
Subcutaneous transplantation
BALB/cAJcl-nu/nu♀9wk
Left：FI 7500
Right：non-stain
in vivo imaging system (IVIS) observation
b
1 × 10⁶ cells/sites
Day 7
Day 14
Day 21
ROI 2=5.660e+08
ROI 2=1.640e+08
ROI 2=1.045e+08
c
2 × 10⁶ cells/sites
Day 7
Day 14
Day 21
ROI 2=1.394e+09
ROI 2=4.023e+08
ROI 2=2.092e+08

432

Figure 5


a
B16F10/EF1a-Luc
cells
stain
0.2 μM FI 7500 30 min 37 ℃
PBS wash 3 times
Subcutaneous
transplantation
Cell suspension 200 μL
BALB/cAJcl-nu/nu♀7 wk
in vivo imaging system
(IVIS) observation
Intraperitoneal
administration of luciferin
b
0 h
1 h
3 h
FI 7500
Luciferin
Epi-Fluorescence
Luminescence
7.0
6.0
5.0
4.0
3.0
2.0
×10⁷
×10⁶

433

Supplementary Files

This is a list of supplementary files associated with this preprint. Click to download.

- SupplementaryFigure1.pptx
- SupplementaryFigure2.pptx
- SupplementaryFigure3.pptx
- SupplementaryFigure4.pptx
- SupplementaryFigure5.pptx